

Kinetics of Scheelite Conversion in Sulfuric Acid

LEITING SHEN,^{1,2} XIAOBIN LI,^{1,3} QIUSHENG ZHOU,¹
ZHIHONG PENG,¹ GUIHUA LIU,¹ TIANGUI QI,¹ and PEKKA TASKINEN²

1.—School of Metallurgy and Environment, Central South University, Changsha 410083, China. 2.—School of Chemical Engineering, Metallurgical Thermodynamics and Modeling Research Group, Aalto University, 02150 Espoo, Finland. 3.—e-mail: x.b.li@csu.edu.cn

Complete conversion of scheelite in H₂SO₄ solution plays a key role in exploration of cleaner technology for producing ammonium paratungstate. In this work, the factors influencing scheelite conversion were investigated experimentally to model its kinetics. The results indicated that the conversion rate increases with increasing temperature and reducing particle size, but is almost independent of stirring speed. Moreover, although the conversion rate increases with increasing initial H₂SO₄ concentration (≤ 1.25 mol/L), it decreases rapidly at 1.5 mol/L H₂SO₄ after 10 min due to formation of a H₂WO₄ layer. The experimental data agree quite well with the shrinking core model under chemical reaction control in ≤ 1.25 mol/L H₂SO₄ solution, and the kinetic equation was established as: $1 - (1 - \alpha)^{1/3} = 222546.6 \cdot C_{\text{H}_2\text{SO}_4}^{1.226} \cdot r_0^{-1} \cdot e^{-\frac{39260}{RT}} \cdot t$ (t , min). This work could contribute to better understanding of scheelite conversion in H₂SO₄ solution and development of a new route for ammonium paratungstate production.

INTRODUCTION

Ammonium paratungstate (APT) is an important intermediate product in industrial tungsten production. The main tungsten minerals in Nature used to produce APT are scheelite (CaWO₄) and wolframite [(Fe,Mn)WO₄], with approximate two-thirds of the world tungsten reserves consisting of scheelite deposits. Due to progressive exhaustion of wolframite sources, scheelite has become the chief raw material for production of tungsten.^{1,2} In APT production, two main methods are used to decompose scheelite, named the soda/caustic soda and acid method.³

The former method decomposes scheelite concentrate in caustic soda or soda solutions by converting CaWO₄ to soluble Na₂WO₄ in an autoclave.^{4,5} This approach has good flexibility for treatment of different types of raw material, such as scheelite concentrates, mixed scheelite–wolframite concentrates, and even low-grade ores. However, this method is usually operated at high temperature and pressure, and in particular requires large amounts of reagents to guarantee high tungsten recovery.^{2,6,7} The resulting sodium tungstate is traditionally converted to ammonium tungstate and excess soda or/and caustic

soda to other sodium salts by solvent extraction or ion exchange in purification of the tungsten-containing solution, raising production costs and environmental stress due to discharge of huge amounts of high-salinity wastewater.⁸

Compared with the soda/caustic soda method, the acid method has the potential to remarkably reduce the discharge of high-salinity wastewater. In this method, acidic medium is used to decompose scheelite concentrates, traditionally forming solid tungstic acid or metatungstate^{9,10} when using HCl/HNO₃, hydrogen aqua oxalato tungstate H₂[WO₃(C₂O₄)H₂O]¹¹ when using H₂C₂O₄, and 12-tungstophosphoric heteropoly acid (H₃PW₁₂O₄₀)¹² when using HCl, H₂SO₄ or HNO₃ in presence of phosphate ion. Considering product costs, equipment corrosion, and operating environment, we have proposed an alternative route based on treatment of scheelite or mixed concentrates in H₂SO₄ solution to form a solid mixture of H₂WO₄ and CaSO₄·*n*H₂O followed by extraction of tungsten in aqueous ammonium carbonate solution.^{13,14} Undoubtedly, complete conversion of scheelite in H₂SO₄ solution is a prerequisite for achieving high tungsten recovery, hence it is important to better understand its conversion kinetics.

Although many researchers have studied the kinetics of scheelite decomposition in mineral acids, they mainly focused on the process without formation of tungstic acid; For instance, Refs. ⁹ and ¹⁰ studied the kinetics of leaching synthetic scheelite in hydrochloric acid or nitric acid with formation of soluble metatungstate at pH 1.5–3.0 in the temperature range of about 300–373 K, pointing out that the leaching process accords with the shrinking core model under both chemical and mass-transfer control. References ¹¹, ¹⁵, and ¹⁶ investigated the behavior and kinetics of calcium tungstate decomposition in oxalate acid solution. Additionally, there exist many reports on leaching scheelite using different mineral acids in presence of phosphate with formation of heteropolytungstate salt, for which the shrinking core model and the Avrami equation under chemical reaction control were adopted to describe the leaching process, yielding activation energy values of 52.91–79 kJ mol⁻¹.^{17–20}

As early as 1965, Forward and Vizsolyi proposed decomposition of scheelite using sulfuric acid with subsequent extraction of tungsten from the resultant mixture of insoluble H₂WO₄ and CaSO₄·*n*H₂O by dihydric or polyhydric aliphatic alcohol.²¹ Obviously, this decomposition process is distinctly different from the abovementioned leaching process for formation of soluble tungsten compounds. Unfortunately, there is limited research on scheelite decomposition using H₂SO₄. Our previous work on this decomposition process revealed the formation mechanism of the H₂WO₄ layer which may cover the surface of unreacted tungsten mineral particles and thus hinder reaction progress, but insufficient attention has been paid to the corresponding kinetics to date.¹³

To further optimize this conversion process, it is necessary to investigate the kinetics of scheelite conversion in sulfuric acid. Thus, the effects of stirring speed, sulfuric acid concentration, temperature, and particle size on the conversion rate were examined in this work, then a kinetic model for the conversion was established. The results of this study are expected to contribute to improving the technique for manufacturing APT from scheelite concentrate via the sulfuric acid conversion–ammonium carbonate leaching route.

MATERIALS AND METHODS

Materials

All reagents used in this work were of analytical grade, purchased from Sinopharm Chemical Reagent Co., Ltd. Scheelite concentrate samples, provided by Jiangxi Rare Metals Tungsten Holdings Group Co., Ltd., China, were dried, ground, and sieved to different size fractions (–100/+74 μm, –74/+58 μm, and –58/+45 μm). The WO₃ content in the different size fractions and the x-ray diffraction (XRD) pattern of the scheelite concentrate are presented in supplementary Table SI and Fig. S1, respectively.

Procedures

Conversion experiments were conducted by placing 250 mL sulfuric acid solution into a 500-mL three-necked round-bottomed flask, which was heated thermostatically in a water bath pot. A sample (5 g) was added to the solution when the operating temperature (±0.5 K) was maintained. The slurry was stirred at designated speed using a polytetrafluoroethylene (PTFE)-coated agitator. The resultant slurry from each run was quickly filtered after a certain duration to obtain a cake (converted product), which was used to determine the conversion ratio of scheelite.

Methods

The converted product obtained in each run was added into 100 mL mixed lixivants (0.5 mol/L NaOH and 2.0 mol/L Na₂CO₃), and the slurry was stirred for 1 h to dissolve H₂WO₄ at ambient temperature. Under these conditions, scheelite cannot be decomposed. The leaching solution and residue were obtained by filtration. The residue was washed, then dried at 363 K in an oven for 8 h to obtain the leaching residue sample, followed by weighing on an analytical balance. Subsequently, the WO₃ content in the residue sample and the leaching solution was measured respectively by thiocyanate method²² to reduce the experimental error. Presuming that the H₂WO₄ in the converted product was completely dissolved and the unreacted scheelite was not decomposed at all, the conversion ratio of scheelite to H₂WO₄ in the conversion process can thus be determined using Eq. 1 as the mean of the conversion ratios calculated from the residue sample and leaching solution.

$$\eta(\text{CaWO}_4) = \frac{1}{2} \left[\left(1 - \frac{m_1 \cdot \omega_1}{m_0 \cdot \omega_0} \right) + \frac{C \cdot V}{m_0 \cdot \omega_0} \right] \times 100\% \quad (1)$$

where, $\eta(\text{CaWO}_4)$ is the conversion ratio of scheelite (%), m_0 is the weight of scheelite concentrate ($m_0 = 5$ g), m_1 is the weight of the residue sample (g), ω_0 is the WO₃ content in the scheelite concentrate (wt.%), ω_1 is the WO₃ content in the residue sample (wt.%), C is the WO₃ content in the leaching solution (g/L), and V is the volume of leaching solution (L).

Phase analysis of the scheelite concentrate was performed by x-ray diffractometer (D8-Advance; Bruker) using Cu K_α radiation with step size of 0.0085° at scan rate of 1° min⁻¹. Scanning electron microscopy (Quanta 650; FEI) and energy-dispersive spectrometry (Quantax 200; Bruker) were used to observe the morphology and elemental distributions of the solid product of scheelite conversion in H₂SO₄ solution.

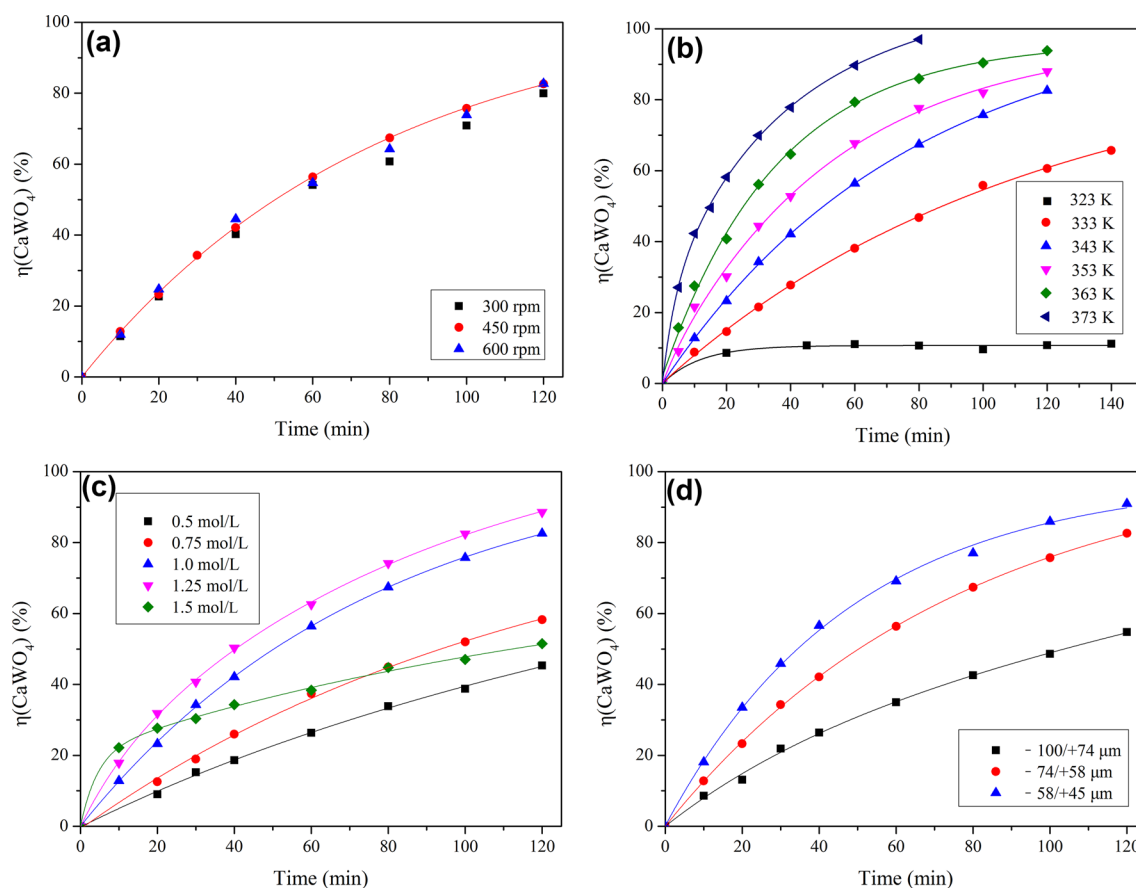


Fig. 1. Effect of the following experimental conditions on scheelite conversion in sulfuric acid. (a) Stirring speed (343 K, 1.0 mol/L H_2SO_4 , particle size $-74/+58 \mu\text{m}$); (b) Temperature (1.0 mol/L H_2SO_4 , 450 rpm, particle size $-74/+58 \mu\text{m}$); (c) H_2SO_4 concentration (343 K, 450 rpm, particle size $-74/+58 \mu\text{m}$); and (d) particle size (343 K, 1.0 mol/L H_2SO_4 , 450 rpm).

RESULTS AND DISCUSSION

Conversion Experiments

The effect of stirring speed on the conversion of scheelite in H_2SO_4 solution was first studied in the range of 300–600 rpm (Fig. 1a). The conversion rate was almost independent of stirring speed in the case of ≥ 450 rpm, indicating that diffusion in bulk solution had no remarkable influence on the scheelite conversion in such situation. Hence, constant stirring speed of 450 rpm was adopted in subsequent experiments, where the conversion may therefore be under chemical reaction control or/and internal diffusion control in the product layer.

The conversion results at different temperatures (323–373 K) are shown in Fig. 1b. It was observed that the scheelite conversion was significantly sensitive to temperature, increasing regularly with increasing temperature. The conversion was only $\sim 10\%$ at 323 K and barely increased after 20 min, whereas almost complete conversion was achieved after 80 min at 373 K.

The effect of H_2SO_4 concentration on scheelite conversion was studied in the range from 0.5 mol/L to 1.5 mol/L. The conversion curves (Fig. 1c) show that the scheelite conversion increased with

increasing sulfuric acid concentration up to 1.25 mol/L. However, when the H_2SO_4 concentration was raised to 1.5 mol/L, the conversion rate decreased rapidly after 10 min and the conversion ratio was only 51.52% even after 120 min, which can be explained by the effect of the H_2SO_4 concentration on the formation of a H_2WO_4 layer on unreacted particles.¹³

The effect of particle size on the conversion of scheelite was also examined using the three sieved samples of scheelite concentrate. The results are presented in Fig. 1d. As expected, reducing the scheelite particle size accelerated the conversion rate of scheelite in H_2SO_4 solution. The tungsten conversion reached 90.9% in 120 min for the $-58/+45 \mu\text{m}$ particles, while it was only about 54.8% for the $-100/+74 \mu\text{m}$ particles.

In summary and as expected, increasing the temperature and reducing the particle size of scheelite facilitated conversion of scheelite in H_2SO_4 solution, while the stirring speed only slightly affected the conversion rate of scheelite at ≥ 450 rpm. The H_2SO_4 solution should have moderate concentration (≤ 1.25 mol/L) to avoid formation of a product layer on unreacted particles.

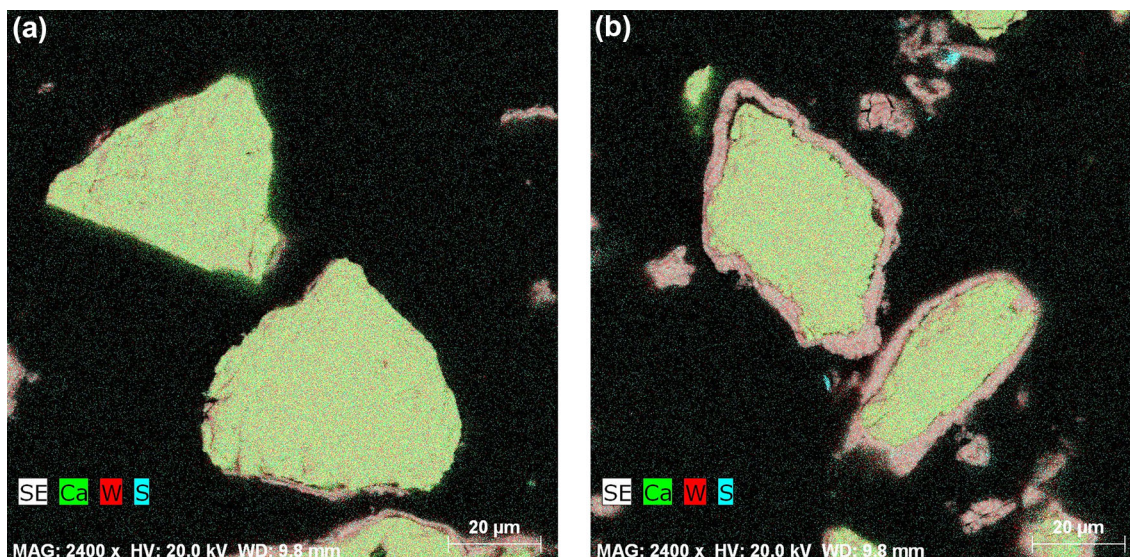


Fig. 2. EDS maps of incompletely converted products (343 K, 60 min, 450 rpm, particle size – 74/+ 58 μm) obtained using (a) 1.0 mol/L and (b) 1.5 mol/L H_2SO_4 .

Kinetic Model Selection

As mentioned above, diffusion through the bulk fluid to the solid particles did not act as the rate-controlling step at stirring speed ≥ 450 rpm. To check the presence of the product layer, EDS mapping of the incompletely converted products obtained in 1.0 mol/L and 1.5 mol/L H_2SO_4 solution was carried out. As shown in Fig. 2, the H_2WO_4 layer was either not observed or found to be discontinuous on the unreacted particles at low H_2SO_4 concentration (1.0 mol/L), whereas the layer was obviously seen and thick in the case of high H_2SO_4 concentration (1.5 mol/L). Moreover, it was also noticed that the nonporous particles reduced from the original size of – 74/+ 58 to < 40 μm . To realize complete conversion of scheelite, it is necessary to avoid formation of a dense H_2WO_4 layer wrapping unreacted particles, thus low H_2SO_4 concentration solution (≤ 1.25 mol/L) is required. Under such conditions, the conversion process is more probably controlled by the chemical surface reaction. Therefore, the shrinking sphere model was chosen to describe the kinetics of scheelite conversion in ≤ 1.25 mol/L H_2SO_4 solution in this work. The equation for surface chemical reaction control according to the shrinking sphere model^{4,23,24} can be written as

$$1 - (1 - \alpha)^{1/3} = K \cdot t \quad (2)$$

For the sake of completeness, the diffusion control through the product layer is also considered, as shown in Eq. 3.

$$1 + 2(1 - \alpha) - 3(1 - \alpha)^{2/3} = K \cdot t \quad \text{or} \quad (3)$$

$$1 - 2/3 \cdot \alpha - (1 - \alpha)^{2/3} = K \cdot t$$

where α represents the conversion ratio of scheelite, K is the overall reaction rate constant (min^{-1}), and t is the reaction time (min).

Kinetic Model Verification

To verify the kinetics model, based on the data in Fig. 1b, the relationships between the conversion ratio (α) of scheelite and reaction time (t) in ≤ 1.25 mol/L H_2SO_4 solution are drawn in Fig. 3a and Supplementary Fig. S2 according to Eqs. 2 and 3, respectively. Obviously, the kinetic data acceptably fit the shrinking sphere model under surface reaction chemical control (Fig. 3a) rather than the internal diffusion control (Supplementary Fig. S2).

Based on the experimental data in Fig. 1c and d, plots of $1 - (1 - \alpha)^{1/3}$ versus reaction time according to Eq. 2 are also illustrated in Fig. 3b and c. The rate constant (K) values obtained in different conditions and the correlation coefficient (R^2) values are listed in Table I, further indicating that the surface reaction chemical-controlled shrinking sphere model fits the kinetic data quite well.

In Eq. 2, the overall reaction rate constant K can be expressed as follows.^{19,25}

$$K = \frac{k \cdot C^n}{r_0 \cdot \rho} \quad \text{with} \quad k = A_0 \cdot \exp\left(-\frac{E}{RT}\right) \quad (4)$$

where k is the rate constant for surface chemical reaction (min^{-1}), C is the concentration of reactant (H_2SO_4 , mol/L), n is the reaction order with respect to

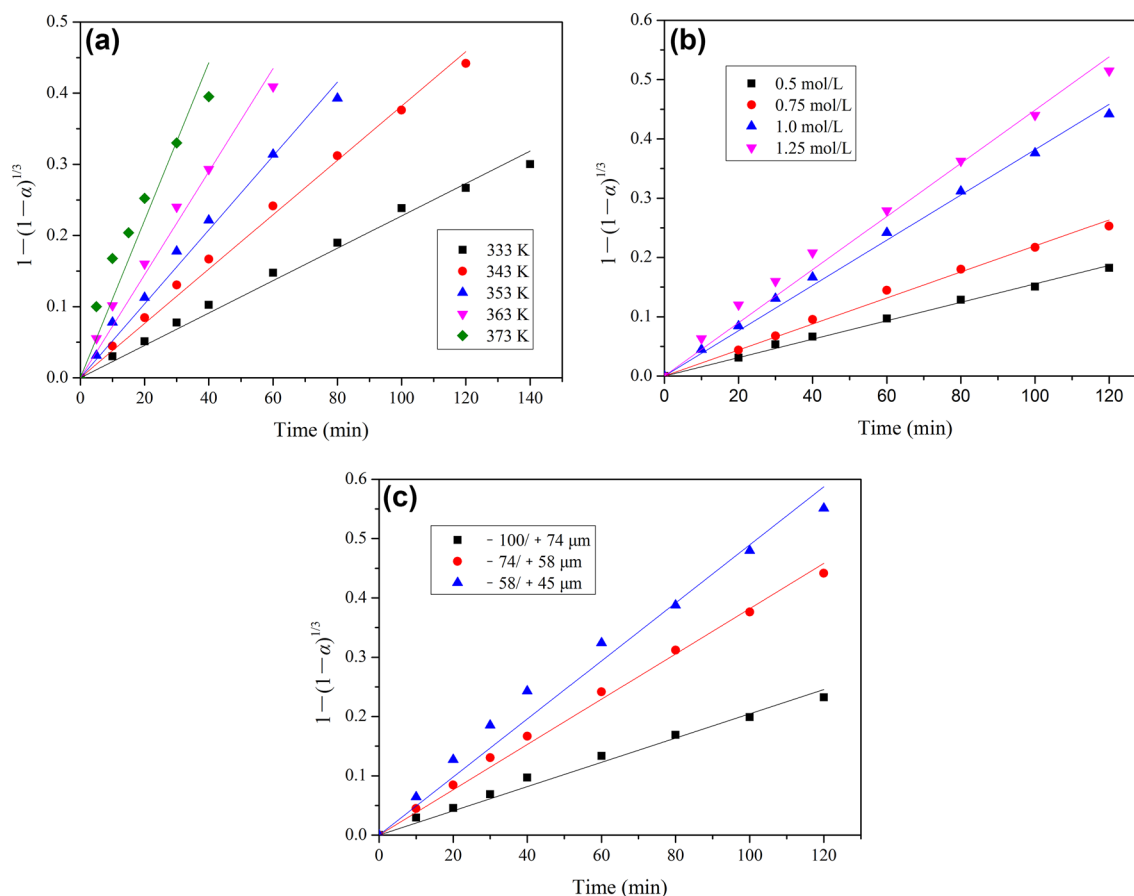


Fig. 3. Plots of $1-(1-\alpha)^{1/3}$ versus time for experimental data from Fig. 1b, c, and d. (a) Effect of temperature. (b) Effect of sulfuric acid concentration. (c) Effect of particle size.

Table I. Apparent rate constant K under different conditions

	Apparent rate constant, K (min^{-1})	Correlation coefficient, R^2
Temperature (K)		
333	0.00228	0.9963
343	0.00382	0.9978
353	0.00519	0.9936
363	0.00724	0.9912
373	0.01107	0.9718
H_2SO_4 concentration (mol/L)		
0.5	0.00155	0.9983
0.75	0.00219	0.9977
1.0	0.00382	0.9978
1.25	0.00449	0.9949
Particle size (μm)		
- 100/+ 74	0.00205	0.9947
- 74/+ 58	0.00382	0.9979
- 58/+ 45	0.00489	0.9911

H_2SO_4 concentration, r_0 is the mean initial particle equivalent radius of scheelite particles (μm), ρ is the density of scheelite (19.3 g/cm^3 at 293 K), A_0 is the

frequency factor (min^{-1}), E is the activation energy (J/mol), R is the universal gas constant ($8.314 \text{ J K}^{-1} \text{ mol}^{-1}$), and T is reaction temperature (K).

The overall reaction rate constants for different temperatures (333–373 K) were determined as the slopes of the straight lines in Fig. 3a. The Arrhenius plot of $\ln K$ versus $1/T$ based on Eq. 4 is depicted in Supplementary Fig. S3a, yielding an activation energy for the conversion reaction of $E = 39.26$ kJ/mol from the slope of the line. The order of reaction with respect to the sulfuric acid concentration (0.5–1.25 mol/L) could also be derived as $n = 1.226$ from the slope of the logarithmic relationship between the overall rate constant K and H_2SO_4 concentration in Supplementary Fig. S3b. As shown in Eqs. 2 and 4, the conversion kinetics is also related to the inverse of the initial particle radius for a chemical reaction-controlled step. Therefore, a plot of K versus $1/r_0$ was drawn (Supplementary Fig. S3c), using the mean of equivalent spherical radiuses. The result shows a favorable zero-intercept linear relationship, further confirming that conversion of scheelite in H_2SO_4 solution is controlled by chemical surface reaction.

According to the discussion above, the kinetic rate equation for the conversion process can be expressed as

$$1 - (1 - \alpha)^{1/3} = \frac{A_0}{\rho} \cdot C_{H_2SO_4}^{1.226} \cdot r_0^{-1} \cdot e^{-\frac{39260}{RT}} \cdot t \quad (5)$$

The overall fit between $1 - (1 - \alpha)^{1/3}$ and $C_{H_2SO_4}^{1.226} \cdot r_0^{-1} \cdot e^{-\frac{39260}{RT}} \cdot t$ for all experimental data from this work is plotted in Supplementary Fig. S3d. A straight line could be well fit to the data points with correlation coefficient above $R^2 = 0.99$, even though some points showed scatter from this line. The value of A_0/ρ was determined as 222,546.6 from the slope of the calculated line. Therefore, the following kinetic expression (Eq. 6) obtained in the present study can be used to reliably describe the conversion process of scheelite in ≤ 1.25 mol/L H_2SO_4 solution:

$$1 - (1 - \alpha)^{1/3} = 222,546.6 \cdot C_{H_2SO_4}^{1.226} \cdot r_0^{-1} \cdot e^{-\frac{39260}{RT}} \cdot t \quad (6)$$

CONCLUSION

Temperature, H_2SO_4 concentration, and particle size markedly affect scheelite conversion in H_2SO_4 solution, whereas the stirring speed has little influence. The obtained experimental data agree well with the shrinking core model, with chemical surface reaction as the rate-controlling step in ≤ 1.25 mol/L H_2SO_4 solution. The apparent activation energy and reaction order with respect to H_2SO_4 concentration were calculated as

$E = 39.26$ kJ/mol and $n = 1.226$, respectively. These results could aid optimization of the scheelite decomposition process in H_2SO_4 solution.

ACKNOWLEDGEMENTS

This work is financially supported by the National Natural Science Foundation of China (Grant No. 51274243).

ELECTRONIC SUPPLEMENTARY MATERIAL

The online version of this article (<https://doi.org/10.1007/s11837-018-2787-2>) contains supplementary material, which is available to authorized users.

REFERENCES

1. E. Lassner, W. Schubert, E. Lüderitz, and H.U. Wolf, *Tungsten, Tungsten Alloys, and Tungsten Compounds. Ullmann's Encyclopedia of Industrial Chemistry* (Weinheim: Wiley, 2012).
2. E. Lassner and W.D. Schubert, *Tungsten: Properties, Chemistry, Technology of the Element, Alloys and Chemical Compounds* (New York: Kluwer Academic, 1999).
3. R.P.S. Gaur, *JOM* 58, 45 (2006).
4. J.P. Martins, *Hydrometallurgy* 42, 221 (1996).
5. Z.W. Zhao, J.T. Li, S.B. Wang, H.G. Li, M.S. Liu, P.M. Sun, and Y.J. Li, *Hydrometallurgy* 108, 152 (2011).
6. J.I. Martins, *Min. Proc. Ext. Met. Rev.* 35, 23 (2014).
7. E. Lassner, *Int. J. Refract. Metals Hard Mater.* 13, 35 (1995).
8. K. Vadasdi, *Int. J. Refract. Metals Hard Mater.* 13, 45 (1995).
9. J.I. Martins, A. Moreira, and S.C. Costa, *Hydrometallurgy* 70, 131 (2003).
10. J.I. Martins, *Ind. Eng. Chem. Res.* 42, 5031 (2003).
11. Y.M. Potashnikov, A.M. Gamol'skii, M.V. Mokhosoev, and F.M. Kozlova, *Zh. Neorg. Khim.* 15, 502 (1970).
12. S. Gurmen, S. Timur, C. Arslan, and I. Duman, *Hydrometallurgy* 51, 227 (1999).
13. X.B. Li, L.T. Shen, Q.S. Zhou, Z.H. Peng, G.H. Liu, and T.G. Qi, *Hydrometallurgy* 171, 106 (2017).
14. L.T. Shen, X.B. Li, Q.S. Zhou, Z.H. Peng, G.H. Liu, T.G. Qi, and P. Taskinen, *JOM* 70, 161 (2018).
15. A.O. Kalpakli, S. Ilhan, C. Kahruman, and I. Yusufoglu, *Hydrometallurgy* 121–124, 7 (2012).
16. A.O. Kalpakli, S. Ilhan, C. Kahruman, and I. Yusufoglu, *Can. Metall. Q.* 52, 348 (2012).
17. G.H. Xuin, D.Y. Yu, and Y.F. Su, *Hydrometallurgy* 16, 27 (1986).
18. C. Kahruman and I. Yusufoglu, *Hydrometallurgy* 81, 182 (2006).
19. W.J. Zhang, J.T. Li, and Z.W. Zhao, *Int. J. Refract. Metals Hard Mater.* 52, 78 (2015).
20. J.T. Li and Z.W. Zhao, *Hydrometallurgy* 163, 55 (2016).
21. F.A. Forward and A.I. Vizsolyi, US Patent No. 3193347 (1965).
22. S.C. Srivastava, S.R. Bhaire, D.N. Wagh, and C.P.S. Iyer, *Bull. Mater. Sci.* 19, 331 (1996).
23. C.Y. Wen, *Ind. Eng. Chem.* 60, 34 (1968).
24. H.Y. Sohn, *Metall. Mater. Trans. B* 35, 121 (2004).
25. Z.W. Zhao, Y. Liang, and H.G. Li, *Int. J. Refract. Metals Hard Mater.* 29, 289 (2011).